

4 × 20 GBPS OFDM BASED ROFSO TRANSMISSION USING HYBRID SCM-MDM UNDER DIFFERENT TURBULENCE CONDITIONS

Ankur SOOD , Rahul KAUSHIK 

Department of Electronics and Communication Engineering, Jaypee Institute of Information Technology, A-10, Sector-62, 201 309 Noida, Uttar Pradesh, India

anksood@yahoo.com, rahul.kaushik@jiit.ac.in

DOI: 10.15598/aeec.v21i1.4656

Article history: Received Aug 04, 2022; Revised Nov 30, 2022; Accepted Dec 21, 2022; Published Mar 31, 2023. This is an open access article under the BY-CC license.

Abstract. A bandwidth efficient Orthogonal Frequency-Division Multiplexing - Radio over Free Space Optics (OFDM-RoFSO) system based on 2-level multiplexing with SCM and MDM domain is implemented. A total of 4-input data streams are multiplexed before being transmitted through RoFSO link. A 4 × 20 Gbps data rate is achieved by performing multiplexing at SCM level with 45 GHz, 60 GHz subcarrier frequencies and then at MDM level with HG01 and LG10 optical modes. With certain design enhancements, channel capacity can be further increased to multi-fold levels. The performance of transmitted input data streams 1-4 is investigated for Bit Error Rate (BER), Q-factor, received signal power, SNR and turbulence conditions under clear air, haze, rain, fog and dust conditions. Eye diagram and electric constellation patterns are analyzed for reliable data transmission. Thus, by using proposed design with 2-level multiplexing, a higher transmission capacity and low crosstalk levels are easily achieved.

Keywords

OFDM, RoFSO, Hermite Gaussian (HG) mode, Laguerre Gaussian (LG) mode, Subcarrier Multiplexing (SCM), Mode Division Multiplexing (MDM)

1. Introduction

In recent times, due to technology enhancement at rapid rate and implementation of 5G network

applications, the demand for multimedia services such as video, live streaming and high-speed internet connectivity is continuously growing. Since there is limited spectrum availability per user, an effective bandwidth utilization is highly required. Therefore, RoFSO technology is proposed to tackle these challenges due to its certain advantages such as license free spectrum, low installation cost, large bandwidth availability and high channel capacity. RoFSO is also preferred due to its flexibility of link establishment in tough geographical terrains and overcrowded areas where fiber installation is not feasible. So, with proper frequency planning, various access points can be deployed using Wireless Local Area Network (WLAN) technology and its practical implementation can be done with RoFSO system [1] and [2].

Beside these advantages, transmission through RoFSO link has certain limitations as well. The optical signal may experience atmospheric attenuation due to rain, haze, fog, dust and snow conditions [3] and [4]. Pointing error and beam wandering also affect the signal performance and limits the overall transmission range [5] and [6]. Experiencing these environmental challenges, existing RoFSO system requires certain design enhancements. Thus, by implementing Orthogonal Frequency Division Multiplexing (OFDM) with RoFSO, signal attenuation levels are reduced drastically. In OFDM, large numbers of orthogonal subcarriers at lower frequencies are utilized for information transmission, thereby reducing ISI and providing low signal attenuation in FSO environment [7].

Information carrying capacity of OFDM based RoFSO system can be enhanced by implementing multiplexing at subcarrier, wavelength, optical modes and

polarization levels. Lim et al. has implemented Sub-carrier Multiplexing (SCM) technique for data transmission through FSO link. With SCM, system BER performance is analyzed for number of users introduced in the system. As the number of users increases, there is a decrease in received signal power levels [8]. Similarly, Mode Division Multiplexing (MDM) using Orbital Angular Momentum (OAM) is another multiplexing technique which offers high channel capacity and has low design complexity. MDM can be used for FSO data transmission for MIMO based systems. Zhang et al. has explained the transmission using MDM for four different optical modes at $l = -3, -2, +2$ and $+3$ which shows minimum signal attenuation and high spectral efficiency [9].

Various optical modes such as HG, LG and LP can be used for signal transmission. Fareed et al. has analysed the performance of various optical modes for a link range of 9 km. Comparative results show that while using LG modes for transmission, minimum BER levels are achieved which indicates minimum Inter-Symbol Interference (ISI) and low signal attenuation [10]. By introducing 2-level multiplexing, channel capacity of RoFSO system can be further improved. A RoFSO system with hybrid Wavelength-Division Multiplexing - Mode Division Multiplexing WDM-MDM scheme is presented here. In this configuration, 4-input data streams having 4×10 Gbps data rate, are utilised for broadband and communication services with radio frequency of 40 GHz [11].

Kakati et al. has explained a 2-level multiplexing scheme using PDM-MDM modes for transmission. A high data rate of 2×320 Gbps is achieved for 16-QAM based OFDM-RoFSO system. Here, Optical modes HG00 and HG01 are used at MDM level and orthogonal polarization is done at PDM level [12]. Furthermore, Singh et al. explained the 16-QAM, OFDM based RoFSO system using combined WDM-PDM modes for transmission. In this design 1.6 Tbps transmission rate is achieved under adverse weather conditions [13]. To further enhance the channel capacity, a 3-level multiplexing using WDM, MDM and PDM for 160 Gbps data transmission was proposed by Huang et al. The results showed a multi-fold increase in channel capacity without affecting its performance in terms of received signal power and show no channel crosstalk levels at receiver output [14]. To further improve the received signal power and BER, the Optical Single Sideband (OSSB) modulation is preferred over Optical Dual Sideband (ODSB) modulation as it minimizes the fading effect for signal transmission through FSO link [15]. Therefore, BER is used to analyze channel performance by observing number of error bits received at output. Also, average BER is derived for analyzing Optical Wireless Communication (OWC) link performance under different turbulence conditions

[16] and [17]. Similarly, for 60 GHz mm wave transmission through FSO link, received signal power levels are compared for optical wavelength of 850 nm and 1550 nm. Comparative results show improved performance while using 1550 nm wavelength for transmission [18].

In the work presented here, a 2-level multiplexing is implemented for OFDM based RoFSO system using Subcarrier Multiplexing (SCM) at level 1 and Mode Division Multiplexing (MDM) at level 2. Information through four data streams is transmitted simultaneously after multiplexing initially at SCM level and then at MDM level.

Using 4-QAM encoder design, each channel is utilized for data carrying capacity of 20 Gbps. So, a total information rate of 80 Gbps is achieved in this design. OSSB modulation is preferred in this design to minimize the fading effect. At SCM level, subcarrier frequencies of 45 GHz and 60 GHz are assigned to input signals. Similarly, at MDM level, HG01 and LG10 optical modes are used for transmission. While integrating above design with OFDM, dual multiplexing of SCM-MDM has not been reported in any of the previous studies. Further, it may be worth noted that by combining SCM with MDM will enhance the overall channel capacity. Therefore, in this work, an attempt has been made to investigate the research work with dual multiplexing of SCM-MDM for various performance parameters.

Section 2. broadly describes OFDM-RoFSO system using 2-level multiplexing. It explains multiplexed RF subcarrier signal at 45 GHz and 60 GHz frequencies using OSSB modulation. It also describes spatial HG01 and LG10 modes at MDM level used as optical carriers for signal transmission through RoFSO link. Section 3. describes a comparative analysis of various optical modes used for transmission and their performance under weak, moderate and strong turbulence conditions for a link range of 500 m to 8,000 m. Concluding remarks are given in Sec. 4.

2. System Model

For an OFDM based RoFSO system, a transmission rate of 80 Gbps is achieved by using 2-level multiplexing while considering four input data streams for transmission. At level 1, Sub-carrier Multiplexing (SCM) with 45 GHz, 60 GHz frequency is carried out. At level-2, Mode Division Multiplexing (MDM) is carried out by considering HG01 and LG10 optical modes for transmission. Data inputs 1-2 and 3-4 are combined at MDM MUX and transmitted through FSO link as shown in Fig. 1 and its simulation set-up is provided in Appendix (Fig. 14). A generalized mathematical

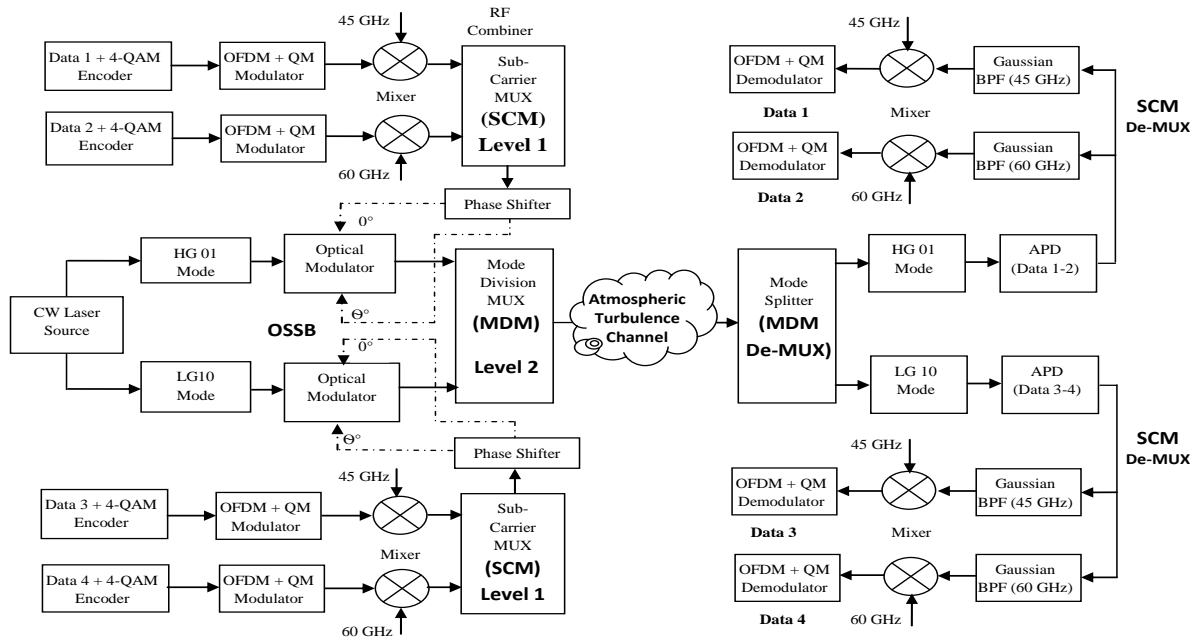


Fig. 1: Schematic of proposed OFDM based RoFSO system using 2-level multiplexing at SCM, MDM levels.

expression for LG modes is given as [11]:

$$\Psi_{m,n}(r, \varphi) = \left(\frac{2r^2}{w_o^2}\right)^{\frac{|n|}{2}} L_m^n\left(\frac{2r^2}{w_o^2}\right) \exp\left(-\frac{r^2}{w_o^2}\right) \cdot \exp\left(j\frac{\pi r^2}{\lambda R_o}\right) \begin{cases} \sin(|n|\varphi), & n \geq 0 \\ \cos(|n|\varphi), & n < 0 \end{cases} \quad (1)$$

where, m and n are mode dependencies on X-index and Y-index representing the azimuth and radial angles, respectively; w_o is the spot size, R represents the radius of curvature and $L_{(n,m)}$ is the Laguerre polynomial.

Similarly, a generalized mathematical expression for HG modes is given as [11]:

$$\Psi_{m,n}(r, \varphi) = H_m\left(\frac{\sqrt{2}x}{w_{ox}^2}\right) \exp\left(-\frac{x^2}{w_{ox}^2}\right) \exp\left(j\frac{\pi x^2}{\lambda R_{ox}}\right) \cdot H_n\left(\frac{\sqrt{2}y}{w_{oy}^2}\right) \exp\left(-\frac{y^2}{w_{oy}^2}\right) \exp\left(j\frac{\pi y^2}{\lambda R_{oy}}\right), \quad (2)$$

where, m and n represent the mode dependencies on X polarization and Y polarization, respectively; H_m and H_n are the Hermite polynomials.

In this system using Pseudo Random Bit Sequence (PRBS) generator, a 20 Gbps data rate is generated and applied at 4-QAM encoder to obtain encoded information bits at its output. The signal is then applied at OFDM modulator which is configured to generate 512 subcarriers at lower frequency having 1024 IFFT points. While using OFDM-RoFSO transmission, the signal experiences minimum channel attenuation at lower frequency levels and reduced Inter-Symbol Interference (ISI). Using quadrature

modulator, I and Q phase components of signal are generated and applied at the mixer stage. At mixer 1, a subcarrier frequency of 45 GHz and at mixer 2, a subcarrier frequency of 60 GHz is mixed with input base-band signal which corresponds to input data streams 1 and 2 respectively. The output RF signal from mixer 1 and mixer 2 are combined to generate SCM signal for data streams 1-2. Similarly, data streams 3-4 are generated by using same SCM parameters.

The SCM signal along with the optical carrier is applied at input ports of DD-MZM as shown in Fig. 1. Here, DD-MZM is customized to generate OSSB modulated signal at its output. In this design, HG01 and LG10 optical modes are considered for transmission. The SCM data streams 1-2 and 3-4 are multiplexed by using MDM-MUX before being transmitted through RoFSO link.

The Free Space Optical (FSO) link equation is given as [15]:

$$P_{rx} = P_{tx} \left[\frac{D_{rx}^2}{(D_{tx} + \theta Z)^2} \right] \eta_{tx} \eta_{rx} \cdot 10^{-\frac{\alpha z}{10}}, \quad (3)$$

where, P_{tx} and P_{rx} are the optical signal power at transmitter and receiver end, respectively; D_{tx} and D_{rx} are the antenna aperture diameters at transmitter and receiver, respectively; θ represents the beam divergence; z is the link distance, the optical efficiency is designated by η_{tx} and η_{rx} and α is the atmospheric attenuation.

Considering clear air attenuation, the signal transmitted between FSO link is analyzed for weak, moderate and strong turbulence conditions. Using Con-

tinuous Wave (CW) laser, spatial profiles of HG01 and LG10 modes are generated as shown in Fig. 2(a) and Fig. 2(b), respectively.

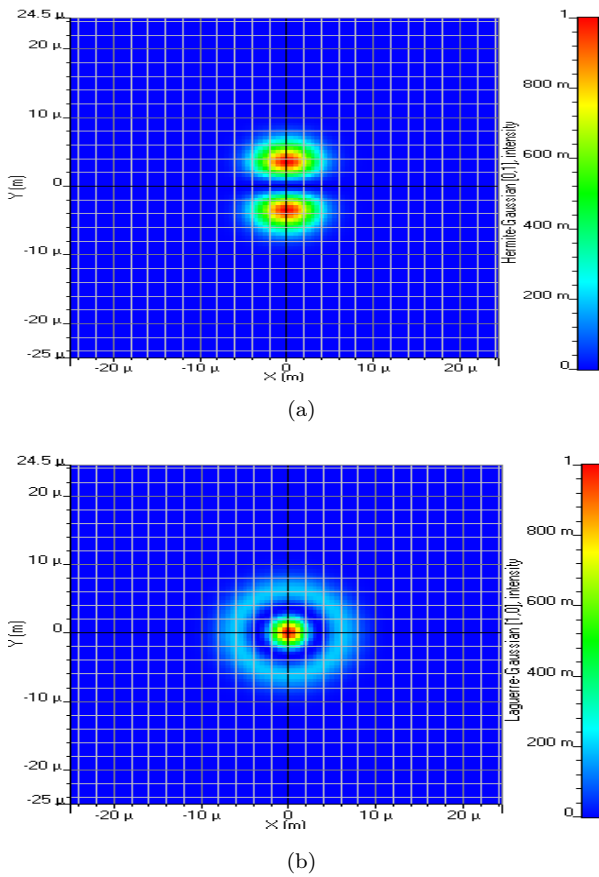


Fig. 2: Spatial profiles of generated optical modes for a) HG01 mode; b) LG10 mode.

The frequency spectrum of RF Subcarrier Multiplexed (SCM) signal at 45 GHz and 60 GHz frequency is shown in Fig. 3.

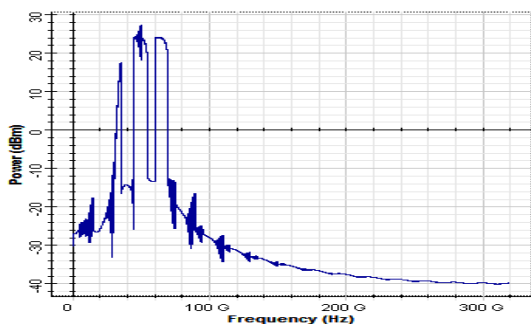


Fig. 3: Spectrum of RF Subcarrier Multiplexed (SCM) signal for data inputs 1–2.

Fig. 4 shows the optical spectrum observed at MDM-MUX output while using HG01 and LG10 as input applied modes.

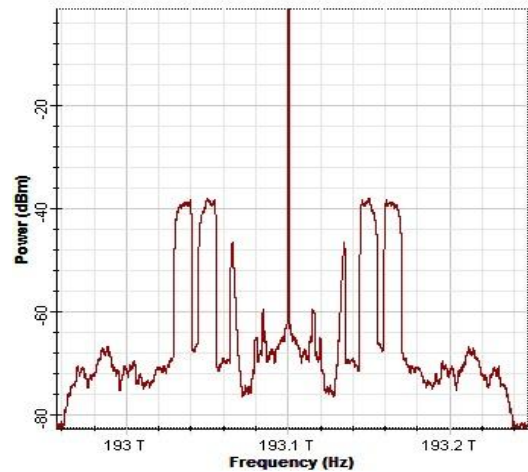


Fig. 4: Measured optical spectrum at MDM MUX output for input data streams 1–2, 3–4.

After multiplexing at MDM level, optically modulated signal is transmitted through RoFSO link. Since optical signal experiences degradation due to atmospheric attenuation and turbulence conditions, its power level can be raised by using an optical amplifier. At receiver, the optical modes are separated by using MDM De-MUX to obtain mode 0 and mode 1 corresponding to HG01 and LG10 modes, respectively. After mode splitting, the optical signal is made to incident on APD detector surface and its electrical equivalent is obtained at the output. The frequency spectrum observed at APD detector output for 45 GHz and 60 GHz subcarrier frequencies is shown in Fig. 5.

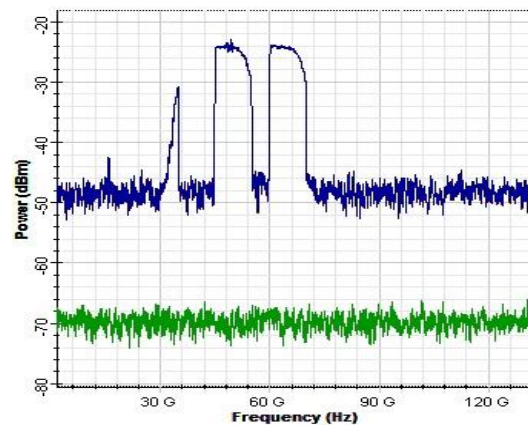


Fig. 5: Spectrum of 45 GHz, 60 GHz information signal at APD detector output for link range, $L = 500$ m and $C_n^2 = 1 \cdot 10^{-15} \text{ m}^{-2/3}$.

The detector output is then processed by the Gaussian band pass filter to separate 45 GHz and 60 GHz subcarrier frequencies. After demodulation, the data streams 1, 2 and 3, 4 corresponding to the optical modes HG01 and LG10 modes, respectively, are obtained at decoder output as shown in Fig. 1.

The receiver simulation circuit is provided in Appendix (Fig. 15). Various system simulation parameters used in this analysis are given in Tab. 1.

Tab. 1: List of simulation parameters.

Parameter	Value
Bit rate	$20 \cdot 10^9$ bits·s ⁻¹
Radio frequency	45 GHz, 60 GHz
No. of subcarriers	512
No. of FFT points	1024
Operating frequency	193.1 THz
Tx. Aperture diameter	5 cm
Beam Divergence	2–6 mrad
Receiver aperture diameter	20 cm
Link length	500 m – 8,000 m
Index refraction structure	$1 \cdot 10^{-15} \text{ m}^{-2/3}$ to $30 \cdot 10^{-15} \text{ m}^{-2/3}$
Wavelength	1550 nm

3. Results and Discussion

The design implementation of OFDM based RoFSO system is carried out with OptiSystem 19.0 version and simulation results are depicted in Fig. 2, Fig. 3, Fig. 4, Fig. 5, Fig. 12 and Fig. 13. The system performance is analyzed for received power, Bit Error Rate (BER), Q-factor etc. while considering various channel parameters, such as link range, atmospheric turbulence and optical modes for FSO transmission. Various transmitter configurations such as:

- Direct transmission without multiplexing i.e. back to back system.
- Subcarrier Multiplexing (SCM-MUX).
- Mode Division Multiplexing (MDM-MUX).
- Hybrid SCM-MDM multiplexing are considered for comparative measurements.

Analysis for received signal power is carried out at APD detector output for various multiplexed design configurations as shown in Fig. 6. In this analysis, comparative results are observed for a link range of up to 8,000 m. The fixed values of system parameters are $\lambda = 1550$ nm, the receiver aperture diameter $D = 20$ cm, $C_n^2 = 1 \cdot 10^{-15} \text{ m}^{-2/3}$ and the beam divergence = 5 mrad. At APD detector output, the observed signal power is -28 dBm, -34 dBm, -39.5 dBm and -44 dBm for back to back system, -31 dBm, -37 dBm, -42 dBm and -46 dBm for SCM-MUX system; -35 dBm, -40.5 dBm, -45.25 dBm and -49.5 dBm for MDM MUX system; and -38 dBm, -43 dBm, -47 dBm and -51 dBm for hybrid SCM-MDM MUX system at a distance of 2,000 m, 4,000 m, 6,000 m and 8,000 m, from transmitter, respectively.

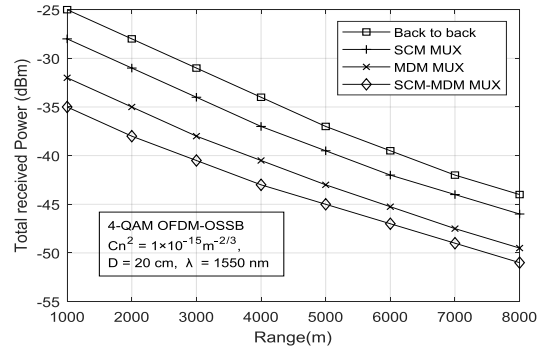


Fig. 6: Plot of received power at APD detector for a link range of up to 8 km using 4-QAM-OFDM-RoFSO system having $C_n^2 = 1 \cdot 10^{-15} \text{ m}^{-2/3}$, $\lambda = 1550$ nm, $D = 20$ cm.

Comparative results in Fig. 6 show that while using dual multiplexed SCM-MDM system, the received signal power is well within the detectable range. Since 4-input data streams are multiplexed in dual SCM-MDM design, a total 80 Gbps transmission rate is achieved, and improved capacity levels are observed. Further, by modifying certain design parameters at SCM and MDM levels, the channel capacity can easily be enhanced.

Similarly, the Q-factor is analysed for various design configurations as shown in Fig. 7. The fixed system parameter values are $\lambda = 1550$ nm, $C_n^2 = 10^{-15} \text{ m}^{-2/3}$, beam divergence = 5 mrad and $D = 20$ cm.

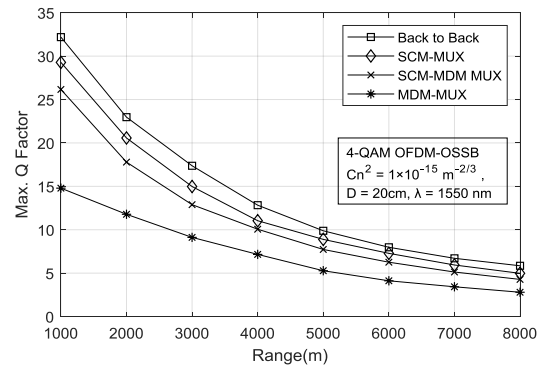


Fig. 7: Q-factor analysis for 4-QAM-OFDM-RoFSO system, considering various multiplexing designs for a link range of up to 8,000 m and a subcarrier frequency of 60 GHz.

The observed Q-factor values are 22.97, 12.83, 7.98 and 5.85 for Back to Back (B2B) system; 20.57, 11.04, 7.28 and 4.98 for SCM-MUX system; 17.79, 10.06, 6.26 and 4.12 for SCM-MDM MUX system; and 11.78, 7.16, 4.12 and 2.8 for MDM-MUX system for a link range of 2,000 m, 4,000 m, 6,000 m and 8,000 m, from transmitter, respectively. The plots observed in Fig. 7 show that the Back to Back (B2B) system has high Q-factor and low interference levels for a link range of 1,000 m to 8,000 m. Since for dual SCM-MDM MUX design, the observed Q-factor values are well within the speci-

fied limits, therefore it can be considered for practical implementation.

Similarly, the performance of OFDM based RoFSO system is analysed for channel crosstalk (XT) while considering SCM, MDM and dual SCM-MDM based configurations. For a multiplexed channel, crosstalk is defined as interference observed from all other channels except the desired channel at receiver. Since the channel crosstalk is measured in terms of BER for a specified Link range (L), a comparative analysis is carried out for various multiplexed configurations, as shown in Fig. 8. The fixed system parameters considered are $\lambda = 1550 \text{ nm}$, $D = 20 \text{ cm}$ and $C_n^2 = 10^{-15} \text{ m}^{-2/3}$.

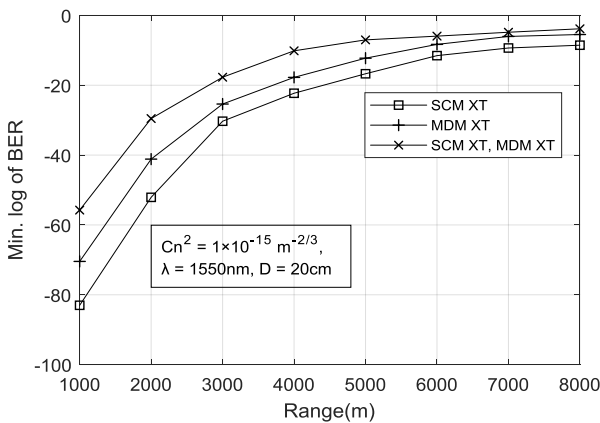


Fig. 8: BER performance measurement for a link range considering weak turbulence for receiver channel with various crosstalk levels.

The plot in Fig. 8 shows that the maximum crosstalk levels are observed for dual SCM-MDM multiplexed system with a maximum BER of $1.48 \cdot 10^{-4}$. Since the BER levels are well within the limits for accurate data transmission, its design implementation can easily be carried out.

It is clear from above findings that channel capacity is improved by using dual multiplexed SCM-MDM system and the results show acceptable received power and channel crosstalk levels. Although the design is capable of transmitting information on four multiplexed channels simultaneously, a further analysis is required to measure individual channel performance. In this design, the channel configurations HG01-45 GHz, LG10-45 GHz, HG01-60 GHz and LG10-60 GHz are used for channels 1–4, respectively. The individual channel performance can be analysed based on BER, SNR, electrical constellation and eye diagram to decide its implementation feasibility in practical environment. The measurements were carried out by considering atmospheric turbulence conditions, link range and atmospheric attenuation.

For a dual multiplexed SCM-MDM system, the BER performance for input data streams 1–4 is analysed for

a link range of up to 8,000 m as shown in Fig. 9. The fixed system parameters are $\lambda = 1550 \text{ nm}$, $D = 20 \text{ cm}$, beam divergence = 5 mrad and $C_n^2 = 1 \cdot 10^{-15} \text{ m}^{-2/3}$. From eye diagram analysis, the observed values of min. log of BER are $-1.41, -1.12, -1.10$ and -1.07 for channel 1; $-1.96, -1.22, -1.12$ and -1.09 for channel 2; $-24.32, -15.13, -9.25$ and -6.44 for channel 3; and $-30.86, -19.45, -12.71$ and -9.73 for channel 4 for a link distance of 2,000 m, 4,000 m, 6,000 m and 8,000 m from transmitter, respectively, as shown in Fig. 9.

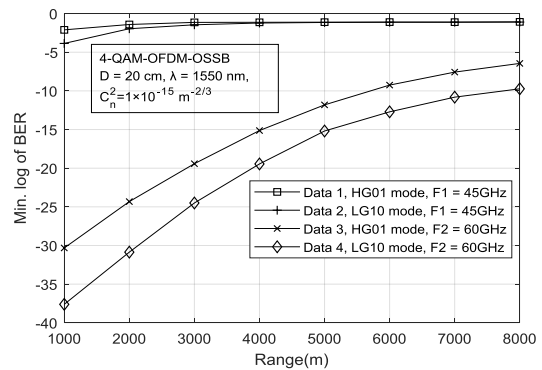


Fig. 9: Estimation of log of BER for a link range of up to 8 km using optical modes HG01 and LG10 at subcarrier frequency of 45 GHz and 60 GHz.

The graphs observed in Fig. 9 show that as the link distance between transmitter and receiver increases, system Bit Error Rate (BER) performance deteriorates. Similarly, the comparative analysis shows that the BER performance is improved while using higher subcarrier frequency of 60 GHz with LG10 and HG01 optical modes for transmission.

So, LG10 and HG01 modes at 60 GHz subcarrier frequency are further analysed by considering various atmospheric turbulence conditions. Scintillation index parameter, C_n^2 values considered for weak, moderate, and strong turbulence conditions are shown in Tab. 2.

Tab. 2: Scintillation index parameter C_n^2 for various turbulence levels.

Turbulence Conditions	Scintillation Model	Scintillation index parameter, C_n^2
Weak	Log-normal	$1 \cdot 10^{-15} \text{ m}^{-2/3}$
Moderate	Log-normal	$9 \cdot 10^{-15} \text{ m}^{-2/3}$
Strong	Gamma-Gamma	$30 \cdot 10^{-15} \text{ m}^{-2/3}$

Fig. 10 shows the performance of HG01 and LG10 modes at 60 GHz subcarrier frequency under different turbulence conditions. The fixed design parameters considered are: $\lambda = 1550 \text{ nm}$, $D = 20 \text{ cm}$ and beam divergence = 5 mrad. For a link distance, $L = 2,000 \text{ m}$, the observed values of min. log of BER are $-50.29, -4.02$ and -2.423 for HG01 mode and $-61.04, -6.20$

and -3.44 for LG10 mode for weak, moderate and strong turbulence conditions, respectively.

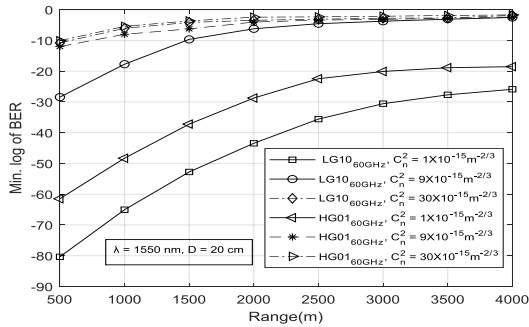


Fig. 10: Estimation of log of BER for weak, moderate and strong turbulence conditions using optical modes HG01 and LG10 at subcarrier frequency of 60 GHz for a link range of up to 4,000 m.

The curves obtained in Fig. 10 show that the transmission using LG10 mode has lower BER in comparison to HG01 mode at 60 GHz subcarrier frequency. Further, analysis shows that under weak turbulence conditions, the system’s BER is low due to minimum signal attenuation as compared to moderate and strong turbulence conditions. Since LG10 mode at 60 GHz subcarrier frequency shows improved channel performance, it can be further analysed by considering various atmospheric attenuation conditions for FSO signal transmission. Attenuation coefficient values considered for the analysis are given in Table. 3.

Tab. 3: Specific atmospheric attenuation coefficients under different weather conditions [3], [4] and [17].

Weather condition	Attenuation (dB·km ⁻¹)
Clear air attenuation	0.0647
Low Haze	1.537
Heavy Haze	10.115
Light Rain	6.27
Heavy Rain	19.28
Thin Fog	9
Heavy Fog	22
Light Dust	25.11
Dense Dust	297.38

The signal performance is mainly affected by atmospheric attenuation due to haze, rain, fog and dust conditions. Fig. 11 shows the performance of LG10 mode at 60 GHz while considering different weather conditions for signal transmission. The system design parameters considered in this analysis are $\lambda = 1550$ nm, $D = 20$ cm, beam divergence equal to 5 mrad and $C_n^2 = 1 \cdot 10^{-15} \text{ m}^{-2/3}$. The observed SNR levels are: 42 dBm, 41 dBm, 40 dBm and 38 dBm for low haze; 40 dBm, 37 dBm, 34 dBm and 30 dBm for light rain; 39 dBm, 36 dBm, 31 dBm and 25 dBm for thin fog; and 36 dBm, 25 dBm, 15 dBm and 0 dBm for light dust for a link range of 500 m, 1,000 m, 1,500 m and 2,000 m from transmitter, respectively, as shown in Fig. 11.

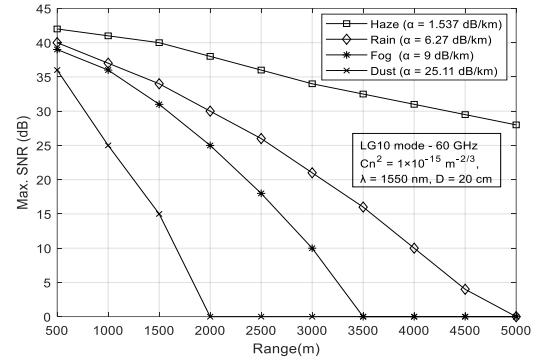


Fig. 11: Observed SNR at APD detector output for haze, rain, fog and dust conditions using 4-QAM-OFDM-RoFSO system for 5,000 m link range, $C_n^2 = 1 \cdot 10^{-15} \text{ m}^{-2/3}$, $\lambda = 1550$ nm, $D = 20$ cm.

Comparative plots in Fig. 11 show quite steady SNR level observed under haze conditions due to low atmospheric attenuation. Since a higher signal attenuation is observed due to rain, fog and dust conditions, the SNR levels deteriorate quite sharply with increase in link distance. Table 4 shows various SNR levels observed under haze, rain, fog and dust conditions.

Tab. 4: Observed SNR levels for different weather conditions.

Range (m)	Atmospheric Attenuation (dB·km ⁻¹)			
	SNR (dBm) under Haze conditions, $\alpha = 1.537$	SNR (dBm) under Rain conditions, $\alpha = 6.27$	SNR (dBm) under Fog conditions, $\alpha = 9$	SNR (dBm) under Dust conditions, $\alpha = 25.11$
500	42	40	39	36
1,000	41	37	36	25
1,500	40	34	31	15
2,000	38	30	25	0
2,500	36	26	18	0
3,000	34	21	10	0
3,500	32.5	16	0	0
4,000	31	10	0	0
4,500	29.5	4	0	0
5,000	28	0	0	0

Figure 12 shows the constellation diagrams of received information streams for channels 1 to 4 with $C_n^2 = 1 \cdot 10^{-15} \text{ m}^{-2/3}$, $\lambda = 1550$ nm. The fixed constellation points show a reliable data transmission of $4 \cdot 20 \text{ Gbits}\cdot\text{s}^{-1}$ for a link range of 2,000 m.

The constellation diagram for LG10 mode at 60 GHz shows more accurate points for reliable transmission as shown in Fig. 12(d). Figure 13 shows the eye diagram patterns observed for channel 1 to 4 while considering a link range of 2,000 m.

Figure 13(d) shows that the transmission using LG10 mode at 60 GHz has clear eye opening which indicates reliable data transmission through RoFSO link and no channel crosstalk levels are observed.

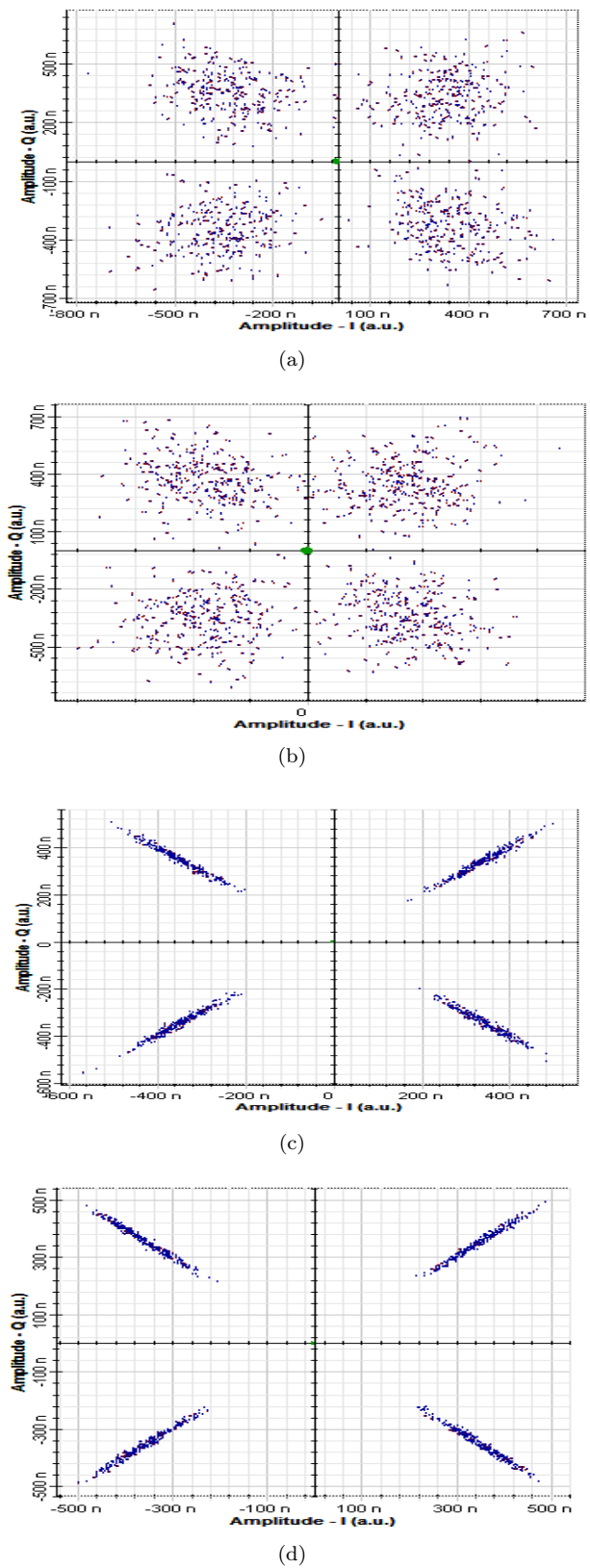


Fig. 12: Constellation diagram of received signal at $L = 2000$ m and $\alpha = 0.0647$ dB·km⁻¹ for a) HG01 mode at 45 GHz, b) LG10 mode at 45 GHz, c) HG01 mode at 60 GHz and d) LG10 mode at 60 GHz.

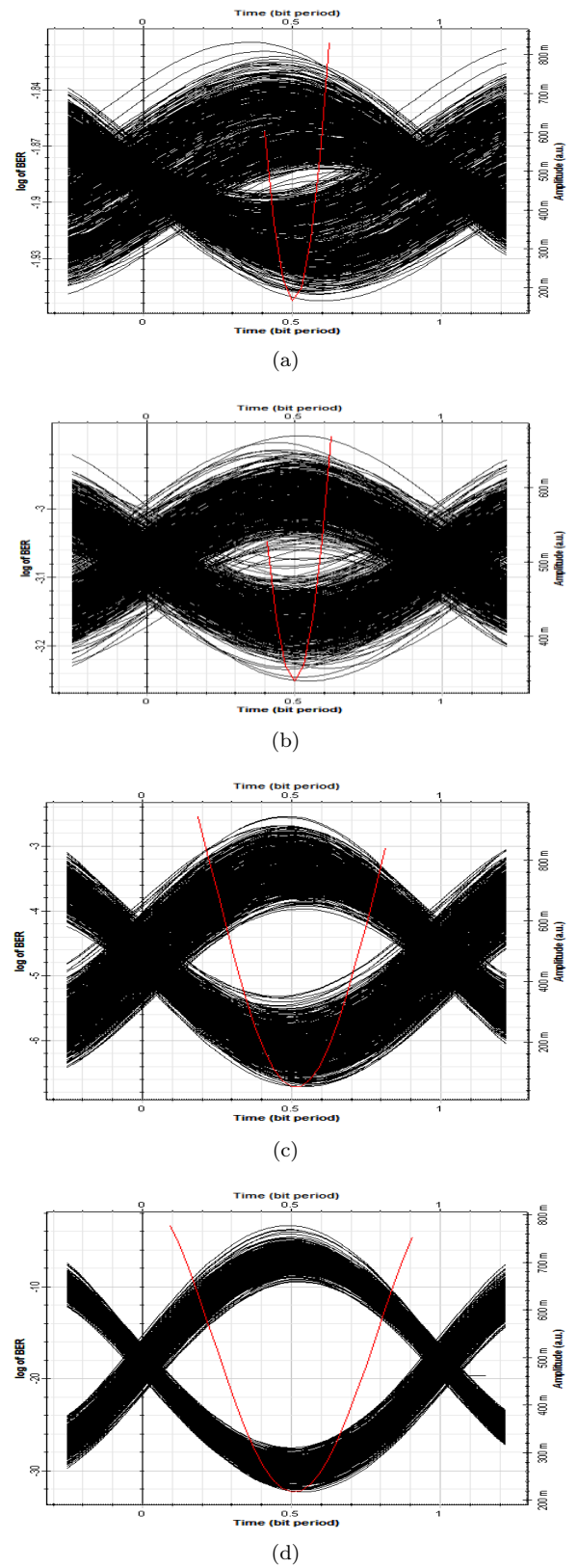


Fig. 13: Eye diagram of received signal for $L = 2000$ m, $\alpha = 0.0647$ dB·km⁻¹ for a) HG01 mode at 45 GHz, b) LG10 mode at 45 GHz, c) HG01 mode at 60 GHz, d) LG10 mode at 60 GHz.

4. Conclusion

In this design, transmission through OFDM-RoFSO system using dual SCM-MDM configuration is implemented. Input data streams 1,2 and 3,4 are multiplexed initially at SCM level with 45 GHz, 60 GHz subcarrier frequencies and then at MDM level (1-2, 3-4) with HG01, LG10 modes before being transmitted through RoFSO link. Since each channel is transmitted with an information carrying capacity of 20 Gbps, a total transmission rate of 80 Gbps ($2 \times 2 \times 20 \text{ Gbit}\cdot\text{s}^{-1}$) is achieved while using 4-input data streams simultaneously.

The FSO channel performance is analysed for a maximum link range of up to 8,000 m under different weather conditions. A comparative analysis based on BER, Q-factor and channel crosstalk is performed for single and dual multiplexed designs with SCM, MDM domains. Satisfactory results are observed for dual SCM-MDM based design. Further, dual SCM-MDM system is analysed for BER and atmospheric turbulence conditions while considering HG01, LG10 modes at 45 GHz and 60 GHz subcarrier frequencies.

Results show significant improvements in received signal power and BER for LG10 mode at higher subcarrier frequency of 60 GHz. Under clear air conditions, FSO channel shows low atmospheric attenuation and improved SNR in comparison to haze, rain, fog and dusty weather conditions. Due to the possibility to accommodate more number of additional information streams with few design change, this approach offers a higher transmission rate, better spectrum efficiency and improved channel capacity levels which can be easily achieved.

Acknowledgment

We express our sincere thanks to Jaypee Institute of Information Technology, Noida, India for providing research facilities and various tools related to the work presented in this design.

Author Contributions

A.S. has developed the design concept, formulated and performed simulation using Optisystem tool and measurements are verified for design feasibility. Both A.S. and R.K. contributed to the final version of the manuscript. R.K. supervised the work done.

References

- [1] MANSOUR, A., R. MASLEH and M. ABAZA. New Challenges in Wireless and Free Space Optical Communications. *Optics and Lasers in Engineering*. 2017, vol. 89, iss. 1, pp. 95–108. ISSN 1873-0302. DOI: 10.1016/j.optlaseng.2016.03.027.
- [2] SALEH, M. A., A. K. ABASS and M. H. ALI. Enhancing performance of WDM-RoFSO communication system utilizing dual channel technique for 5G applications. *Optical and Quantum Electronics*. 2022, vol. 54, iss. 8, pp. 1–11. ISSN 1572-817X. DOI: 10.1007/s11082-022-03857-8.
- [3] ESMAIL, M. A., M. S. FATHALLAH and M. S. ALOUINI. An Experimental Study of FSO Link Performance in Desert Environment. *IEEE Communications Letters*. 2020, vol. 20, iss. 9, pp. 1888–1891. ISSN 1558-2558. DOI: 10.1109/LCOMM.2016.2586043.
- [4] SINGH, M. and S. N. POTTOO, J. MALHOTRA, A. GROVER and M. ALY. Millimeter-wave hybrid OFDM-MDM radio over free space optical transceiver for 5G services in desert environment. *Alexandria Engineering Journal*. 2021, vol. 60, iss. 5, pp. 4275–4285. ISSN 2090-2670. DOI: 10.1016/j.aej.2021.03.029.
- [5] HASAN, M. Z., M. J. HOSSAIN, J. CHENG and V. C. M. LEUNG. Subcarrier Intensity Modulated Optical Wireless Communications: A Survey from Communication Theory Perspective. *ZTE Communications*. 2016, vol. 14, iss. 2, pp. 2–12. ISSN 1673-5188. DOI: 10.3969/j.issn.1673-5188.2016.02.001.
- [6] VITASEK, J., E. LEITGEB, T. DAVID, J. LATAL and S. HEJDUK. Misalignment loss of Free Space Optic link. In: *2014 16th International Conference on Transparent Optical Networks (ICTON)*. Graz: IEEE, 2014, pp. 1–5. ISBN 978-1-4799-5601-2. DOI: 10.1109/ICTON.2014.6876494.
- [7] BOFFI, P., P. MARTELLI, P. PAROLARI, L. BLUNDETTO, J. MOROSI and G. CINCOTTI. Demonstration and Performance Investigation of Hybrid OFDM Systems for Optical Access Network Applications. *IEEE Photonics Journal*. 2015, vol. 7, iss. 1, pp. 1–9. ISSN 1943-0655. DOI: 10.1109/JPHOT.2014.2381651.
- [8] LIM, W., T. S. CHO, C. YUN, and K. KIM. Average BER analysis of SCM-based free-space optical systems by considering the effect of IM3 with OSSB signals under turbulence channels. *Optics Express*. 2009, vol. 17, iss. 23, pp. 20721–20726. ISSN 1094-4087. DOI: 10.1364/OE.17.020721.

- [9] ZHANG, W., S. ZHENG, X. HUI, R. DONG, X. JIN, H. CHI and X. ZHANG. Mode Division Multiplexing Communication Using Microwave Orbital Angular Momentum: An Experimental Study. *IEEE Transactions on Wireless Communications*. 2017, vol. 16, iss. 2, pp. 1308–1318. ISSN 1558-2248. DOI: 10.1109/TWC.2016.2645199.
- [10] FAREED, A., A. GHAZI, A. A. DAWOODI, S. A. ALJUNID, S. Z. S. IDRUS, C. B. M. RASHIDI, A. AMPHAWAN, A. M. FAKHRUDEEN and I. E. IFADHEL. Comparison of Laguerre-Gaussian, Hermite-Gaussian and linearly polarized modes in SDM over FMF with electrical nonlinear equalizer. In: *The 2nd International Conference on Applied Photonics and Electronics 2019 (InCAPE 2019)*. Putrajay: AIP Publishing, 2019, pp. 1–9. ISBN 978-0-7354-1954-4. DOI: 10.1063/1.5142137.
- [11] LIANG, P., C. ZHANG, J. NEBHEN, S. CHAUDHARY and X. TANG. Cost-Efficient Hybrid WDM-MDM-Ro-FSO System for Broadband Services in Hospitals. *Frontier in Physics*. 2021, vol. 9, iss. 1, pp. 1–7. ISSN 2296-424X. DOI: 10.3389/fphy.2021.732236.
- [12] KAKATI, D. and R. K. SONKAR. A 2×320 Gbps Hybrid PDM-MDM-OFDM system for High Speed Terrestrial FSO Communication. In: *2020 Conference on Lasers and Electro-Optics Pacific Rim (CLEO-PR)*. Sydney: IEEE, 2020, pp. 1–2. ISBN 978-1-7281-4333-0. DOI: 10.1364/CLEOPR.2020.C5F_3.
- [13] SINGH, M., J. MALHOTRA, A. ATIEH, H. J. EL-KHOZONDAR and V. DHASARATHAN. Performance Investigation of 1.6 Tbps Hybrid WDM-PDM-OFDM based Free Space Optics Transmission Link. *Wireless Personal Communications*. 2021, vol. 117, iss. 3, pp. 2285–2309. ISSN 1572-834X. DOI: 10.1007/s11277-020-07972-1.
- [14] HUANG, H., G. XIE, Y. YAN, N. AHMED, Y. REN, Y. YUE, D. ROGAWSKI, M. J. WILLNER, B. I. ERKMEN, K. M. BIRNBAUM, S. J. DOLINAR, M. P. J. LAVERY, M. J. PADGETT, M. TURAND and A. E. WILLNER. 100 Tbit/s free-space data link enabled by three-dimensional multiplexing of orbital angular momentum, polarization, and wavelength. *Optics Letters*. 2014, vol. 39, iss. 2, pp. 197–200. ISSN 1539-4794. DOI: 10.1364/OL.39.000197.
- [15] SOOD, A. and R. KAUSHIK. Performance Analysis of 20 Gbps-60 GHz OFDM-RoFSO Transmission with ODSB and OSSB Modulation Using Hybrid Mode. In: *2021 7th International Conference on Signal Processing and Communication (ICSC)*. Noida: IEEE, 2021, pp. 85–90. ISBN 978-1-6654-2739-5. DOI: 10.1109/ICSC53193.2021.9673279.
- [16] KAUSHIK, R., V. KHANDELWAL and R. C. JAIN. An Approximation for BER of Optical Wireless System under Weak Atmospheric Turbulence using Point Estimate. *Journal of Optical Communications*. 2017, vol. 40, iss. 4, pp. 473–479. ISSN 2191-6322. DOI: 10.1515/joc-2017-0119.
- [17] LATAL, J., L. HAJEK, A. VANDERKA, J. VITASEK, P. KOUDELKA and S. HEIDUK. Real Measurements and Evaluation of the Influence of Atmospheric Phenomena on FSO Combined with Modulation Formats. *Electronics*. 2020, vol. 20, iss. 2, pp. 62–68. ISSN 1450-5843. DOI: 10.7251/ELS1620062L.
- [18] SOOD, A. and R. KAUSHIK. BER Analysis of 60GHz Millimeter Wave Over Free Space Optical Communication System. In: *2020 6th International Conference on Signal Processing and Communication (ICSC)*. Noida: IEEE, 2020, pp. 29–33. ISBN 978-1-7281-5493-0. DOI: 10.1109/ICSC48311.2020.9182756.

About Authors

Ankur SOOD received his B.E. in Electronics from Swami Ramanand Teerth Marathwada University, Nanded, in 2001 and M.E. in Electronics and Telecommunication Engineering from Government College of Engineering, Pune in 2003. He is currently pursuing Ph.D. from Jaypee Institute of Information Technology, Noida, India. His areas of interest include Free Space Optics and Radio over FSO (RoFSO) communication systems.

Rahul KAUSHIK received his B.Tech. (Electronics and Telecommunication Engineering) and M.Tech. (Electronics Engineering) from University of Allahabad, India in 2001 and 2003, respectively. He received his Ph.D. Degree from Jaypee Institute of Information Technology (JIIT), Noida, India, in 2017. Presently, he is working as associate professor in the department of Electronics & Communication Engineering (ECE) at JIIT, Noida, India. His research interests lie in the areas of Optical Communication. He is a member of OPTICA, senior member of Institute of Electrical and Electronics Engineers (IEEE) and a fellow of Institution of Electronics and Telecommunication Engineers (IETE), India.

